




## Programmed twisting of phenylene–ethynylene linkages from aromatic stacking interactions†

Cite this: *J. Mater. Chem. C*, 2019, 7, 1198

William J. Mullin,<sup>a</sup> Robert H. Pawle,<sup>a</sup> Seth A. Sharber,<sup>a</sup> Peter Müller<sup>b</sup> and Samuel W. Thomas III \*<sup>a</sup>

Control over the conformation and packing of conjugated materials is an unsolved problem that prevents the rational design of organic optoelectronics, such as preventing self-quenching of luminescent molecules. Exacerbating this challenge is a general lack of widely applicable strategies for controlling packing with discrete, directional non-covalent interactions. Here, we present a series of conjugated molecules with diverse backbones of three or four arenes that feature pentafluorobenzyl ester substituents. Nearly all the compounds reveal intramolecular stacking interactions between the fluoroarene (ArF) side-chains and non-fluorinated arenes (ArH) in the middle of the chromophores; a twisted PE linkage accompanies each example of this intramolecular ArF–ArH stacking. Furthermore, these molecules can resist dramatic changes to emission upon transition from organic solution to thin film when ArF rings prevent interchromophore interactions. By broadening the structural space of conjugated backbones over which ArF–ArH stacking can twist PE linkages reliably and prevent self-quenching of solids with simple synthetic approaches, this work suggests fluorinated benzyl ester substituents adjacent to phenylene ethynylene linkages as supramolecular synthons for the crystal engineering of organic optoelectronic materials.

Received 8th November 2018,  
Accepted 17th December 2018

DOI: 10.1039/c8tc05612a

rscl.li/materials-c

### Introduction

Conjugated small molecules are important components of organic electronic devices that enable tuning of optoelectronic properties with changes of their chemical structure.<sup>1</sup> Among the expanding panoply of conjugated moieties, phenylene ethynylenes (PEs) are well-established yet unique molecules that possess backbones of alternating arenes and triple bonds. Solid-state PEs have applications in sensing,<sup>2–4</sup> anti-microbial coatings,<sup>5–7</sup> nanoelectronics,<sup>8–10</sup> and photovoltaic cells.<sup>11–13</sup> These compounds adopt wide ranges of conformations along their conjugated backbones due to low barriers of rotation, which can be as small as 1 kcal mol<sup>−1</sup>.<sup>14,15</sup> Although this shallow energy surface makes controlling solid-state conformations and luminescence challenging, it also presents opportunities for responsive materials, as the optoelectronic properties of conjugated molecules depend strongly on conformation.<sup>16–18</sup>

Several approaches exist for controlling PE backbone conformations *via* modifications to the main chain in order to bias luminescent properties. Covalent tethering between the two

arenes in elaborated tolans can lock twisted conformations to achieve phosphorescence,<sup>19,20</sup> while steric interactions bias PE torsions and prevent intermolecular aggregation.<sup>21,22</sup> Several related strategies use directional non-covalent interactions between moieties installed into PE backbones,<sup>23,24</sup> but this can restrict the types of main-chain arenes that can participate. A notable example is intramolecular hydrogen bonds that increase the co-planarity of PEs in solution.<sup>25</sup> Overall, however, the purposeful integration of discrete, directional non-covalent interactions to engineer solid-state packing of conjugated materials is relatively rare, especially those involving non-conjugated pendant groups.

The large number of arenes present in conjugated materials frequently means that their interactions<sup>26</sup> dictate solid-state packing.<sup>27</sup> While edge-to-face interactions of benzene dimers are electrostatically favorable, the opposing electronic distribution of perfluorinated arenes and non-fluorinated arenes yields cofacial interactions (ArF–ArH stacking) as a generally applicable design motif in crystal engineering.<sup>28,29</sup> These cofacial aromatic interactions present the advantage of easily tunable strengths through Hammett-type electronic substituent effects. Examples of their influence include fluorinated acenes such as pentacene<sup>30</sup> and rubrene,<sup>31</sup> which cofacially stack, strongly deviating from the classic “herringbone” packing of acenes that features edge–face interactions.

Our group has used directional ArF–ArH stacking to control both the conformation and packing of solid PEs.<sup>32–34</sup> In this approach, stacking interactions between (i) fluorinated benzyl

<sup>a</sup> Department of Chemistry, Tufts University, 62 Talbot Ave., Medford, MA 02155, USA. E-mail: sam.thomas@tufts.edu

<sup>b</sup> Department of Chemistry, MIT, 77 Massachusetts Ave., Cambridge, MA 02139, USA

† Electronic supplementary information (ESI) available: NMR spectra, optical spectra, and crystallographic details. CCDC 1875124–1875132. For ESI and crystallographic data in CIF or other electronic format see DOI: 10.1039/c8tc05612a

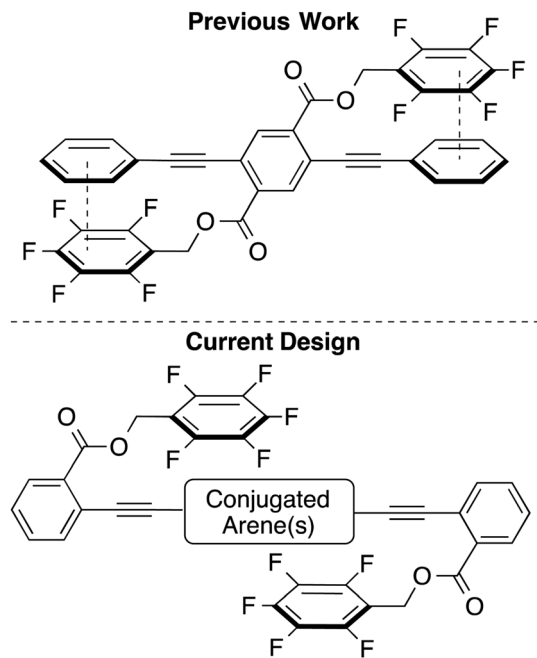


Fig. 1 Comparison of general molecular structures in which ArF–ArH stacking interactions twist PE backbones in our previous work (top), and the more general design of molecules presented herein (bottom).

substituents on a central dibenzylterephthalate and (ii) terminal rings of a 3-ring PE facilitate twisting of the PE backbones and prevent chromophore aggregation. In several publications that focus exclusively on this common molecular core (Fig. 1), we demonstrated that electronic substituent effects dictate whether stacking interactions occur,<sup>33</sup> as well as tunable reversible mechanofluorochromism based on the lengths of alkyl substituents.<sup>34</sup>

The potential generality of these directional ArF–ArH interactions to control solid-state conformations of PEs, however, remains an open question. Our objective in this work is to broaden the applicability of such stacking interactions between conjugated arenes and pendant fluorinated rings to program twisted PE linkages, and to demonstrate such control as an approach to improve the predictability of their solid-state luminescence. To this end, we have incorporated perfluorinated benzyl esters into PEs composed of up to four aromatic rings along their conjugated backbones, with a greater diversity of conjugated chemical linkages beyond alkynes and easily installed terminal rings bearing fluoroarene pendants for intramolecular stacking. These molecules display diverse intermolecular and intramolecular packing as a result of ArF–ArH stacking interactions, and show prominent twisted PE linkages in their crystal structures, which in some cases dictate different solid state optical properties depending on the extent of electronic coupling that the twisting enables.

## Experimental section

All reactants and solvents were purchased from commercial sources and used without further purification. Syntheses requiring

air free conditions were performed using standard Schlenk techniques under an argon atmosphere. Flask column chromatography was performed using silica gel (230–400 mesh). NMR spectra were acquired on a Bruker Avance III 500 or a Bruker DPX-300 spectrometer. UV/visible absorbance and fluorescence spectra were acquired for target compounds in dilute chloroform solution and thin films. UV/visible absorbance spectra were acquired using a Varian Cary-100 spectrophotometer, employing quartz cuvettes and glass microscope slides for solution and thin film measurements, respectively. Fluorescence emission and excitation spectra were acquired using a PTI Quantum Master 4 equipped with a 75 W Xe lamp and a time-correlated single photon-counting module. Relative quantum yields in dilute solution were determined using quinine sulfate in 0.1 M sulfuric acid and anthracene in ethanol as standards using values reported by Melhuish.<sup>35</sup> Single crystals for X-ray diffraction analysis were grown by evaporation of solvent from chloroform solutions, or from diffusion of hexanes into a solution of the compound in chloroform. Single crystal diffraction data were collected using a Bruker D8 Quest diffractometer coupled to a photon CMOS detector with Mo K $\alpha$  radiation ( $\lambda = 0.71073 \text{ \AA}$ ).

Compounds **1** and **3** were prepared according to a previously reported procedure.<sup>36</sup> A solution of pentafluorobenzyl alcohol or benzyl alcohol (5.25 mmol) in dichloromethane (60 mL) was added to a round bottom flask containing 2-iodobenzoic acid (5 mmol), dimethylaminopyridine (1 mmol), and dicyclohexylcarbodiimide (5.5 mmol). The reaction mixture was stirred for 16 hours at room temperature, then filtered over a bed of Celite, and rinsed with diethyl ether. The resulting organic solution was washed with water and brine, dried over MgSO<sub>4</sub>, filtered, and concentrated *in vacuo*. The crude product was purified by flash column chromatography on silica, using dichloromethane as the eluent.

**1:** Obtained as a colorless solid in 75% yield. <sup>1</sup>H NMR (300 MHz, CDCl<sub>3</sub>):  $\delta$  7.98 (d, 1H), 7.7 (d, 1H), 7.34 (t, 1H), 7.16 (t, 1H), 5.44 (s, 2H). <sup>13</sup>C NMR (125 MHz, CDCl<sub>3</sub>):  $\delta$  165.6, 145.9 (d,  $J = 252 \text{ Hz}$ ), 142.2 (d,  $J = 252 \text{ Hz}$ ), 141.5, 137.6 (d,  $J = 252 \text{ Hz}$ ), 134.0, 133.1, 131.2, 128.0, 109.1, 94.2, 54.2.

**3:** Obtained as a colorless oil in 90% yield. <sup>1</sup>H NMR (300 MHz, CDCl<sub>3</sub>):  $\delta$  7.99 (d, 1H), 7.82 (d, 1H), 7.49–7.34 (m, 6H), 7.13 (t, 1H), 5.38 (s, 2H), in agreement with the literature.<sup>36</sup> Compounds **2** and **4** were prepared by modifying a previously reported procedure and executed in air-free conditions.<sup>36</sup> 40 mL of degassed 4:1 THF:NET<sub>3</sub> (v/v) was added to a round-bottom flask containing compound **1** or **3** (1 eq., 3.0 mmol), bis(triphenylphosphine)palladium(II) dichloride (0.05 equiv., 0.15 mmol) and copper(I) iodide (0.05 equiv., 0.15 mmol) under argon. Trimethylsilylacetylene (TMSA, 1.1 equiv., 3.3 mmol) was then added, and the reaction mixture was stirred for 16 hours at room temperature. Solvents were removed *in vacuo* and the crude product was purified by flash column chromatography on silica gel, using 2:1 CH<sub>2</sub>Cl<sub>2</sub>:hexanes as the eluent and TMS deprotection was carried out.

**TMS-alkyne derived from 1.** Obtained as an orange solid in 86% yield. <sup>1</sup>H NMR (500 MHz, CDCl<sub>3</sub>):  $\delta$  7.89 (d, 1H), 7.61 (d, 1H), 7.48 (t, 1H), 7.37 (t, 1H), 5.47 (s, 2H), 0.28 (s, 9H).

$^{13}\text{C}$  NMR (125 MHz,  $\text{CDCl}_3$ ):  $\delta$  165.3, 145.7 (d,  $J = 252$  Hz), 142.0 (d,  $J = 252$  Hz), 137.4 (d,  $J = 252$  Hz), 134.9, 131.9, 131.1, 130.4, 128.2, 123.7, 102.9, 100.5, 53.8,  $-0.3$ .

**TMS-alkyne derived from 3.** Obtained as an orange oil in 85% yield.  $^1\text{H}$  NMR (300 MHz,  $\text{CDCl}_3$ ):  $\delta$  7.92 (d, 1H), 7.59 (d, 1H), 7.46–7.35 (m, 7H), 5.39 (s, 2H), 0.23 (s, 9H), in agreement with the literature.<sup>36</sup> Each TMS-alkyne (1 equiv., 2.0 mmol) was dissolved in 10 mL of THF and cooled in an ice-water bath. Tetrabutylammonium fluoride (TBAF, 1.1 equiv., 2.2 mmol) was added as a 1.0 M solution in THF, and the reaction mixture was stirred for ten minutes. The reaction mixture was then poured into water, and the product was extracted with diethyl ether, dried over  $\text{MgSO}_4$ , filtered, and concentrated *in vacuo* to yield a black residue. The crude product was purified by flash column chromatography on silica gel using 1 : 1  $\text{CH}_2\text{Cl}_2$  : hexanes as the eluent.

**2:** Obtained as a pink solid in 61% yield.  $^1\text{H}$  NMR (300 MHz,  $\text{CDCl}_3$ ):  $\delta$  7.90 (d, 1H), 7.62 (d, 1H), 7.49 (t, 1H), 7.39 (t, 1H), 5.45 (s, 2H), 3.35 (s, 1H).  $^{13}\text{C}$  NMR (125 MHz,  $\text{CDCl}_3$ ):  $\delta$  165.1, 145.0 (d,  $J = 252$  Hz), 141.8 (d,  $J = 252$  Hz), 137.5 (d,  $J = 252$  Hz), 135.1, 132.2, 131.4, 130.5, 128.5, 122.9, 109.4, 82.6, 81.6, 53.9.

**4:** Obtained as a light pink oil in 62% yield.  $^1\text{H}$  NMR (300 MHz,  $\text{CDCl}_3$ ):  $\delta$  7.97 (d, 1H), 7.62 (d, 1H), 7.48–7.31 (m, 7H), 5.38 (s, 2H), 3.35 (s, 1H), in agreement with the literature.<sup>36</sup>

**4,4'-Diiodotolane** (dihalide intermediate for **4-PE** compounds) was prepared according to a previously reported procedure as follows:

**4,4'-Diaminotolane.** Following to a modified reported procedure,<sup>10</sup> executed under air- and water-free conditions, a 4 : 1 (v/v) THF : triethylamine mixture (5 mL) was sparged with argon and added to a round bottom flask containing 4-ethynylaniline (1 equiv., 1.28 mmol), 4-iodoaniline (1 equiv., 1.28 mmol), bis(triphenylphosphine)palladium(II) dichloride (0.05 equiv., 0.064 mmol) and copper(I) iodide (0.05 equiv., 0.064 mmol). The resulting dark mixture was stirred overnight at room temperature under argon, while wrapped in aluminum foil. The reaction mixture was then poured into 10 mL of deionized water and extracted with  $\text{CH}_2\text{Cl}_2$  ( $3 \times 25$  mL). The combined organic layers were dried over magnesium sulfate, filtered, and concentrated *in vacuo* to yield a dark oily solid. The crude product was purified by flash column chromatography on silica, using 2%  $\text{NEt}_3$  in  $\text{CH}_2\text{Cl}_2$  to 5%  $\text{NEt}_3$  in  $\text{CH}_2\text{Cl}_2$  as the eluent to yield 4,4'-diaminotolane as an orange solid in 56% yield.  $^1\text{H}$  NMR (300 MHz, acetone- $d_6$ ):  $\delta$  7.39 (d, 4H), 6.45 (d, 4H), 3.66 (bs, 4H), consistent with the literature.<sup>10</sup>

**4,4'-Diiodotolane.** Following a modified version of a previously reported procedure,<sup>37</sup> 4,4'-diaminotolane (1 equiv., 0.72 mmol) was suspended in 2.5 mL of 20% aqueous  $\text{H}_2\text{SO}_4$  and cooled in an ice bath. A solution of  $\text{NaNO}_2$  (2.25 equiv., 1.62 mmol) in 1 mL of  $\text{H}_2\text{O}$  was added to the suspension. After 30 minutes, the resulting orange solution was added in portions to a solution of KI (10.5 equiv., 7.58 mmol) in 2 mL of  $\text{H}_2\text{O}$ . More  $\text{H}_2\text{O}$  was added to promote stirring, and the mixture was stirred for 2 hours. The mixture was filtered, and the precipitate was washed with  $\text{H}_2\text{O}$  and then with dilute aqueous sodium thiosulfate solution to yield 4,4'-diiodotolane as a light brown solid in 45% yield.  $^1\text{H}$  NMR (500 MHz,  $\text{CDCl}_3$ ):  $\delta$  7.71 (d, 4H), 7.28 (d, 4H), consistent with a

previous report.<sup>37</sup> 4,4'-Diiodo-2,2',6,6'-tetramethylbiphenyl (dihalide intermediate for **4-TMBP-F5**) was prepared according to a previously reported procedure as follows:<sup>38</sup>

**1,2-Bis(3,5-dimethylphenyl)hydrazine.** A suspension of 1,3-dimethyl-5-nitrobenzene (1 equiv., 13.2 mmol), zinc powder (5.8 equiv., 77 mmol), and EtOH (8 mL) was heated to reflux over 30 minutes. A solution of sodium hydroxide (5.7 equiv., 75 mmol) in water (10 mL) was added dropwise to the zinc suspension, resulting in an orange solution with suspended zinc. Heating was continued at reflux overnight, while more zinc powder (2.0 g) was added in portions over the first 4 hours. The hot suspension was then filtered over a bed of Celite into a solution of sodium bisulfite (200 mg) in 30% aqueous acetic acid (30 mL), and the filter cake was rinsed with hot EtOH. The slurry was cooled in an ice bath and filtered, yielding an orange solid, which was recrystallized from heptane to yield the desired product as pale orange needles in 75% yield.  $^1\text{H}$  NMR (500 MHz,  $\text{CDCl}_3$ ):  $\delta$  6.52 (s, 6H), 5.50 (s, 2H), 2.27 (s, 12H), consistent with a previous report.<sup>38</sup>

**4,4'-Diamino-2,2',6,6'-tetramethylbiphenyl.** 1,2-Bis(3,5-dimethylphenyl)hydrazine (1 equiv., 3.32 mmol) was added to 10% HCl (40 mL), and the reaction mixture was heated at reflux. After 2 hours, all of the starting material had dissolved, and  $^1\text{H}$  NMR spectra showed the consumption of the starting material. The reaction mixture was cooled to room temperature and the pH was raised to  $>10$  with 1 M NaOH. The product was extracted using diethyl ether, washed with water and brine, dried over  $\text{MgSO}_4$ , filtered, and concentrated *in vacuo* to afford a red/orange oil, which solidified upon storage, to yield the desired product in 93% yield. This material was used without further purification.  $^1\text{H}$  NMR (300 MHz,  $\text{CDCl}_3$ ):  $\delta$  6.47 (s, 4H), 3.52 (s, 4H), 1.81 (s, 12H), consistent with a previous report.<sup>38</sup>

**4,4'-Diiodo-2,2',6,6'-tetramethylbiphenyl.** A solution of  $\text{NaNO}_2$  (2.2 equiv., 4.35 mmol) in water (2 mL) was added to a suspension of 4,4'-diamino-2,2',6,6'-tetramethylbiphenyl (1 equiv., 1.94 mmol) and 33% aqueous  $\text{H}_2\text{SO}_4$  (12 mL) in an ice bath. After approximately 30 min, the starting material had dissolved, and the reaction mixture was transferred to a solution of  $\text{I}_2$  (2.8 equiv., 5.32 mmol) and NaI (4.7 equiv., 9 mmol) in water (2.5 mL) at  $0^\circ\text{C}$ . 10 mL of water and 25 mL of  $\text{CH}_2\text{Cl}_2$  were added, and the reaction mixture was stirred overnight at room temperature. Sodium thiosulfate (1 g) was added and the reaction mixture was stirred for an additional 30 minutes. The mixture was filtered, resulting in a two-phase filtrate that was separated. The aqueous phase was extracted with chloroform, and the combined organic phases were washed with 10% aqueous sodium thiosulfate solution and brine, dried over  $\text{MgSO}_4$ , filtered, and concentrated *in vacuo* to yield a dark yellow solid. The crude product was purified by flash column chromatography on silica, using hexanes as the eluent, to yield the desired product as a colorless solid in 42% yield.  $^1\text{H}$  NMR (300 MHz,  $\text{CDCl}_3$ ):  $\delta$  7.48 (s, 4H), 1.83 (s, 12H), consistent with a previous report.<sup>38</sup>

### General Procedure for Sonogashira reactions

The reaction solvent of 5 : 1 THF :  $\text{NEt}_3$  (v/v) or 1 : 1 THF :  $\text{NEt}_3$  was deoxygenated by sparging with argon for 20 minutes and

added to a round bottom flask containing 2 or 4 (2.1 equiv.), diiodide core (1 equiv.), copper(i) iodide (0.05 equiv.), and bis(triphenylphosphine)palladium(II) dichloride (0.05 equiv.) under argon, and stirred overnight. The reaction was monitored by TLC, and completion was judged based on the consumption of the diiodide. Solvents were then removed *in vacuo*, and the resulting crude product was purified by flash column chromatography and recrystallization, details of which are described for each target compound below.

**4-BP-F5.** **4-BP-F5** was prepared according to the general Sonogashira procedure, using 1.53 mmol of 2, 0.70 mmol of 4,4'-diiodobiphenyl, 0.035 mmol of  $\text{Cl}_2\text{Pd}(\text{PPh}_3)_2$ , 0.035 mmol of CuI, and 30 mL of 5 : 1 THF :  $\text{NEt}_3$ . 1 : 1  $\text{CH}_2\text{Cl}_2$  : hexanes was used as the chromatography eluent, and the product was recrystallized from hexanes in 44% yield.  $^1\text{H}$  NMR (500 MHz,  $\text{CDCl}_3$ ):  $\delta$  8.04 (d, 2H), 7.68 (d, 2H), 7.62 (d, 2H), 7.58–7.53 (m, 6H), 7.44 (t, 2H), 5.50 (s, 4H).  $^{13}\text{C}$  NMR (125 MHz,  $\text{CDCl}_3$ ):  $\delta$  165.5, 145.7 (d,  $J = 252$  Hz), 141.5 (d,  $J = 252$  Hz), 140.5, 137.5 (d,  $J = 252$  Hz), 134.2, 132.3, 131.8, 131.0, 130.6, 128.1, 126.9, 124.0, 122.3, 109.3, 94.3, 88.8, 53.9.

**4-BT-F5.** **4-BT-F5** was prepared according to the general Sonogashira procedure, using 0.82 mmol of 2, 0.41 mmol of 4,4'-diiodobithiophene, 0.02 mmol of  $\text{Cl}_2\text{Pd}(\text{PPh}_3)_2$ , 0.02 mmol of CuI, and 24 mL of 5 : 1 THF :  $\text{NEt}_3$ . 1 : 1  $\text{CH}_2\text{Cl}_2$  : hexanes was used as the chromatography eluent. **4-BT-F5** was recrystallized from acetone/water in 63% yield.  $^1\text{H}$  NMR (500 MHz,  $\text{CDCl}_3$ ):  $\delta$  8.03 (d, 2H), 7.65 (d, 2H), 7.54 (t, 2H), 7.43 (t, 2H), 7.17 (d, 2H), 7.13 (d, 2H).  $^{13}\text{C}$  NMR (125 MHz,  $\text{CDCl}_3$ ):  $\delta$  165.2, 145.8 (d,  $J = 252$  Hz), 141.8 (d,  $J = 252$  Hz), 137.5 (d,  $J = 252$  Hz), 138.6, 134.0, 133.1, 132.3, 131.0, 130.3, 128.3, 124.1, 123.5, 122.4, 109.3, 93.2, 87.7, 54.0.

**4-DMF-F5.** **4-DMF-F5** was prepared according to the general Sonogashira procedure, using 0.26 mmol of 2, 0.13 mmol of 2,7-diiodo-9,9-dimethylfluorene, 0.007 mmol of  $\text{Cl}_2\text{Pd}(\text{PPh}_3)_2$ , 0.007 mmol of CuI, and 12 mL of 5 : 1 THF :  $\text{NEt}_3$ . 1 : 1  $\text{CH}_2\text{Cl}_2$  : hexanes was used as the chromatography eluent, and **4-DMF-F5** was then recrystallized from acetone/water in 75% yield.  $^1\text{H}$  NMR (500 MHz,  $\text{CDCl}_3$ ):  $\delta$  8.02 (d, 2H), 7.74–7.69 (m, 4H), 7.63 (s, 2H), 7.56 (t, 2H), 7.49–7.41 (m, 4H), 5.52 (s, 4H), 1.57 (s, 6H).  $^{13}\text{C}$  NMR (125 MHz,  $\text{CDCl}_3$ ):  $\delta$  165.4, 154.1, 145.7 (d,  $J = 252$  Hz), 141.7 (d,  $J = 252$  Hz), 139.0, 137.5 (d,  $J = 252$  Hz), 134.2, 132.3, 130.84, 130.8, 130.5, 128.0, 125.8, 124.2, 122.0, 120.2, 109.4, 95.5, 88.3, 53.9, 47.0, 26.8.

**4-TMBP-F5.** **4-TMBP-F5** was prepared according to the general Sonogashira procedure, using 0.11 mmol of compound 9, 0.24 mmol of 2, 0.01 mmol of  $\text{Cl}_2\text{Pd}(\text{PPh}_3)_2$ , 0.01 mmol of CuI, and 6 mL of 5 : 1 THF :  $\text{NEt}_3$ . 1 : 1  $\text{CH}_2\text{Cl}_2$  : hexanes was used as the chromatography eluent, and **4-TMBP-F5** was recrystallized from acetone/water in 43% yield.  $^1\text{H}$  NMR (500 MHz,  $\text{CDCl}_3$ ):  $\delta$  7.99 (d, 2H), 7.65 (d, 2H), 7.51 (t, 2H), 7.38 (t, 2H), 7.27 (s, 4H), 5.49 (s, 4H), 1.91 (s, 12H).  $^{13}\text{C}$  NMR (125 MHz,  $\text{CDCl}_3$ ):  $\delta$  165.5, 145.8 (d,  $J = 252$  Hz), 141.8 (d,  $J = 252$  Hz), 140.3, 137.5 (d,  $J = 252$  Hz), 135.8, 134.4, 132.2, 130.8, 130.63, 130.4, 127.8, 124.3, 121.6, 109.5, 95.1, 87.3, 54.0, 19.5.

**3-DBPE-F5.** **3-DBPE-F5** was prepared according to the general Sonogashira procedure, using 0.23 mmol of compound 2,

0.11 mmol of 1,4-dibutoxy-2,5-diiodobenzene, 0.006 mmol of  $\text{Cl}_2\text{Pd}(\text{PPh}_3)_2$ , 0.006 mmol of CuI, and 10 mL of 1 : 1 THF :  $\text{NEt}_3$ . 1 : 1  $\text{CH}_2\text{Cl}_2$  : hexanes was used as the chromatography eluent, and **3-DBPE-F5** was recrystallized from chloroform/methanol in 54% yield.  $^1\text{H}$  NMR (500 MHz,  $\text{CDCl}_3$ ):  $\delta$  8.00 (d, 2H), 7.69 (d, 2H), 7.55 (t, 2H), 7.41 (t, 2H), 7.02 (s, 2H), 4.05 (t, 4H), 1.87 (quin, 4H), 1.57 (sext, 4H), 1.00 (t, 6H).  $^{13}\text{C}$  NMR (125 MHz,  $\text{CDCl}_3$ ):  $\delta$  165.2, 153.7, 145.7 (d,  $J = 252$  Hz), 141.7 (d,  $J = 252$  Hz), 137.5 (d,  $J = 252$  Hz), 134.4, 132.2, 130.7, 130.3, 127.9, 124.5, 116.9, 114.2, 109.4, 93.2, 91.5, 69.4, 53.8, 31.4, 19.2, 13.9.

**4-PE-F5.** **4-PE-F5** was prepared according to the general Sonogashira procedure, using 0.26 mmol of 2, 0.13 mmol of compound 6, 0.007 mmol of  $\text{Cl}_2\text{Pd}(\text{PPh}_3)_2$ , 0.007 mmol of CuI, and 12 mL of 5 : 1 THF :  $\text{NEt}_3$ . 1 : 1  $\text{CH}_2\text{Cl}_2$  : hexanes was used as the chromatography eluent, and **4-PE-F5** was recrystallized from acetone/water in 75% yield.  $^1\text{H}$  NMR (500 MHz,  $\text{CDCl}_3$ ):  $\delta$  8.02 (d, 2H), 7.67 (d, 2H), 7.58–7.41 (m, 12H), 5.50 (s, 4H).  $^{13}\text{C}$  NMR (125 MHz,  $\text{CDCl}_3$ ):  $\delta$  165.3, 145.9 (d,  $J = 252$  Hz), 141.8 (d,  $J = 252$  Hz), 137.5 (d,  $J = 252$  Hz), 134.2, 132.3, 131.5, 131.4, 130.9, 130.6, 128.2, 123.8, 123.3, 123.1, 109.3, 94.2, 91.0, 89.8, 54.0.

**4-PE-H5.** **4-PE-H5** was prepared according to the general Sonogashira procedure, using 0.55 mmol of 4, 0.25 mmol of compound 6, 0.013 mmol of  $\text{Cl}_2\text{Pd}(\text{PPh}_3)_2$ , 0.013 mmol of CuI, and 12 mL of 5 : 1 THF :  $\text{NEt}_3$ . 1 : 1  $\text{CH}_2\text{Cl}_2$  : hexanes was used as the chromatography eluent, and **4-PE-H5** was recrystallized from acetone/water in 22% yield.  $^1\text{H}$  NMR (500 MHz,  $\text{CDCl}_3$ ):  $\delta$  8.06 (d, 2H), 7.68 (d, 2H), 7.56–7.49 (m, 10H), 7.44–7.36 (m, 12H), 5.45 (s, 4H).  $^{13}\text{C}$  NMR (125 MHz,  $\text{CDCl}_3$ ):  $\delta$  166.1, 135.8, 134.2, 131.9, 131.7, 131.5, 130.8, 128.6, 128.4, 128.3, 128.2, 123.6, 123.3, 123.0, 94.1, 91.1, 90.3, 67.2.

**3-PE-F5.** **3-PE-F5** was prepared according to the general Sonogashira procedure, using 0.48 mmol of 2, 0.24 mmol of 1,4-diiodobenzene, 0.012 mmol of  $\text{Cl}_2\text{Pd}(\text{PPh}_3)_2$ , 0.012 mmol of CuI, and 12 mL of 5 : 1 THF :  $\text{NEt}_3$ . 1 : 1  $\text{CH}_2\text{Cl}_2$  : hexanes was used as the chromatography eluent, and **3-PE-F5** was recrystallized from acetone in 61% yield.  $^1\text{H}$  NMR (500 MHz,  $\text{CDCl}_3$ ):  $\delta$  8.02 (d, 2H), 7.69 (d, 2H), 7.56 (t, 2H), 7.48 (s, 4H), 7.43 (t, 2H), 5.5 (s, 4H).  $^{13}\text{C}$  NMR (125 MHz,  $\text{CDCl}_3$ ):  $\delta$  165.3, 145.8 (d,  $J = 252$  Hz), 141.8 (d,  $J = 252$  Hz), 137.5 (d,  $J = 252$  Hz), 134.3, 132.3, 131.4, 130.9, 130.6, 128.2, 123.8, 123.3, 109.4, 94.2, 89.8, 53.9.

**3-PE-H5.** **3-PE-H5** was prepared according to the general Sonogashira procedure, using 0.67 mmol of 4, 0.33 mmol of 1,4-diiodobenzene, 0.02 mmol of  $\text{Cl}_2\text{Pd}(\text{PPh}_3)_2$ , 0.02 mmol of CuI, and 12 mL of 5 : 1 THF :  $\text{NEt}_3$ . 3 : 1  $\text{CH}_2\text{Cl}_2$  : hexanes was used as the chromatography eluent, and **3-PE-H5** was recrystallized from acetone/water in 70% yield.  $^1\text{H}$  NMR (500 MHz,  $\text{CDCl}_3$ ):  $\delta$  8.02 (d, 2H), 7.65 (d, 2H), 7.53–7.28 (m, 18H).  $^{13}\text{C}$  NMR (75 MHz,  $\text{CDCl}_3$ ):  $\delta$  166.1, 135.8, 134.2, 131.9, 131.7, 131.6, 130.8, 128.6, 128.4, 128.3, 128.2, 123.6, 123.2, 94.2, 90.2, 67.1.

## Results and discussion

### Molecular design and synthesis

In contrast to our previous three-ring PEs that twist in response to ArF–ArH interactions of a central terephthalate with

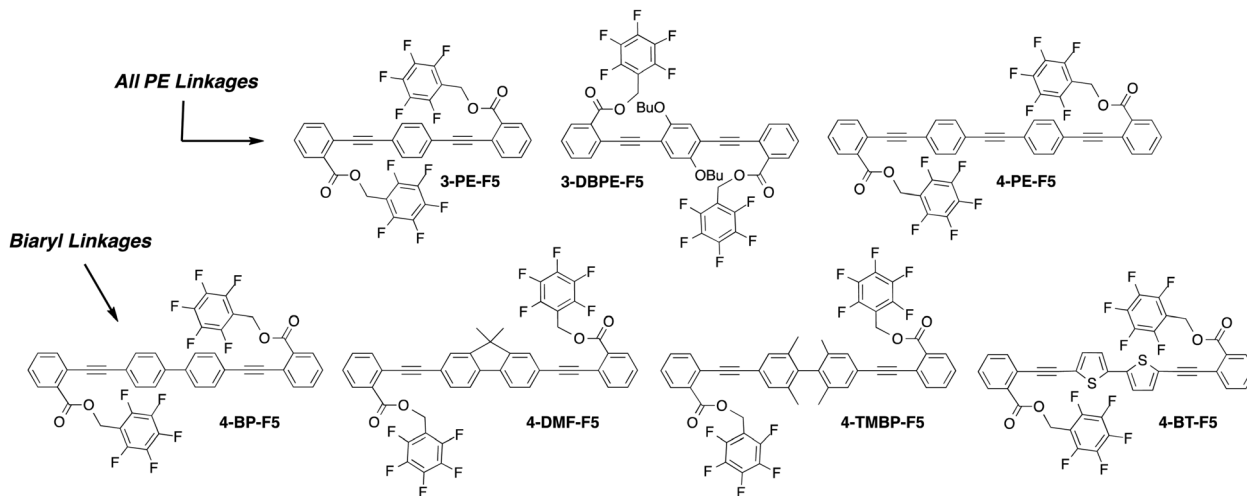


Fig. 2 Seven pentafluorobenzyl benzoate-substituted PEs studied in this work.

fluorinated benzyl esters, the molecules presented herein comprise pentafluorobenzyl *o*-ethynylbenzoate esters attached to both termini of a conjugated core (Fig. 1). With the hypothesis that intramolecular ArF–ArH stacking would twist the PE linkages, we prepared and determined crystal structures for seven such molecules, which had either three or four conjugated arenes as the “main chains” of the chromophores (Fig. 2). Scheme 1 shows how we prepared *o*-ethynyl benzyl benzoates **2** (perfluorobenzyl) and **4** (benzyl): esterification of 2-iodobenzoic acid with perfluorobenzyl alcohol or benzyl alcohol yielded esters **1** and **3**, followed by Sonogashira cross-coupling with trimethylsilylacetylene and subsequent deprotection of the trimethylsilyl group with tetrabutylammonium fluoride yielded the common ethynyl intermediates **2** and **4**. Sonogashira reactions between these alkynes and various dihalides, which were either commercially

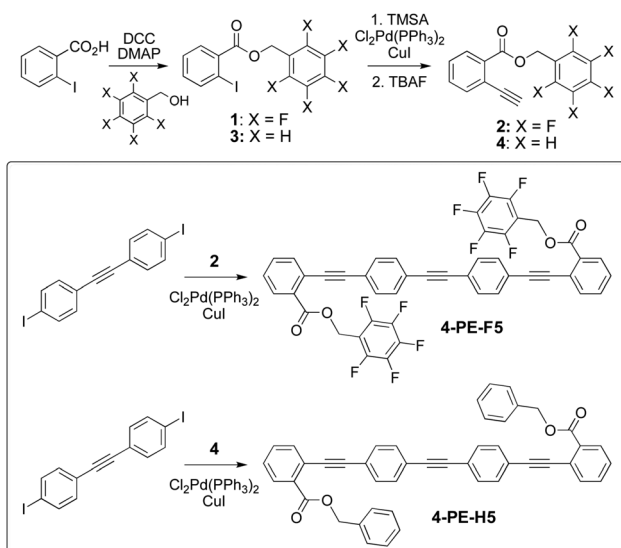
available or prepared according to literature procedures, provided the target compounds shown in Fig. 2. We grew X-ray quality single crystals for each of these molecules.

### X-ray crystallography

**Molecules with only PE linkages.** We first sought to establish the viability of our design in Fig. 1 for broadening the applicability of this approach to controlling solid conjugated materials. We hypothesized that the same key components in this different configuration would, within three-ring and four-ring PEs: (i) participate in intramolecular ArF–ArH stacking interactions and (ii) induce twisting of PEs with such stacking interactions. As described below, the crystal structures of the PEs described herein strongly support the potential generality of this design by showing intramolecular cofacial ArF–ArH stacking, with each instance of this stacking yielding a twisted PE linkage.

The simplest molecule we investigated is **3-PE-F5**, which comprises an unsubstituted central PE ring flanked on each side by pentafluorobenzyl benzoates. The crystal structure shows that only one of these two ArF rings participates in both intramolecular and intermolecular ArF–ArH slipped-stacks with central PE rings, each with closest contacts between carbon atoms <3.4 Å. These stacking interactions form infinite slipped columns along the crystallographic *a*-axis, along which infinite slip-stacked interactions between the benzoate rings also extend. Importantly, the PE linkage across which the ArF–ArH cofacial interactions occur is twisted, with a torsional angle of 67°, while the other PE linkage is coplanar (<10° torsions); instead of intramolecular stacking interactions, the two faces of this ArF ring: (i) stack with benzoate rings of another molecule and (ii) interact with the edge of an ArF ring of another molecule.

An analogous PE is **3-DBPE-F5**, which has two *n*-butoxy substituents on the central ring. Intramolecular cofacial ArF–ArH interactions of similar configuration figure prominently in this structure, with each face of the electron-rich dialkoxy ring stacking with one of the ArF rings, with a closest C··C contact of 3.47 Å between the rings (Fig. 3). The opposite, outward-pointing



Scheme 1 Synthesis of ethynyl intermediates **2** and **4** and representative couplings to prepare conjugated molecules with potential for intramolecular aromatic interactions.

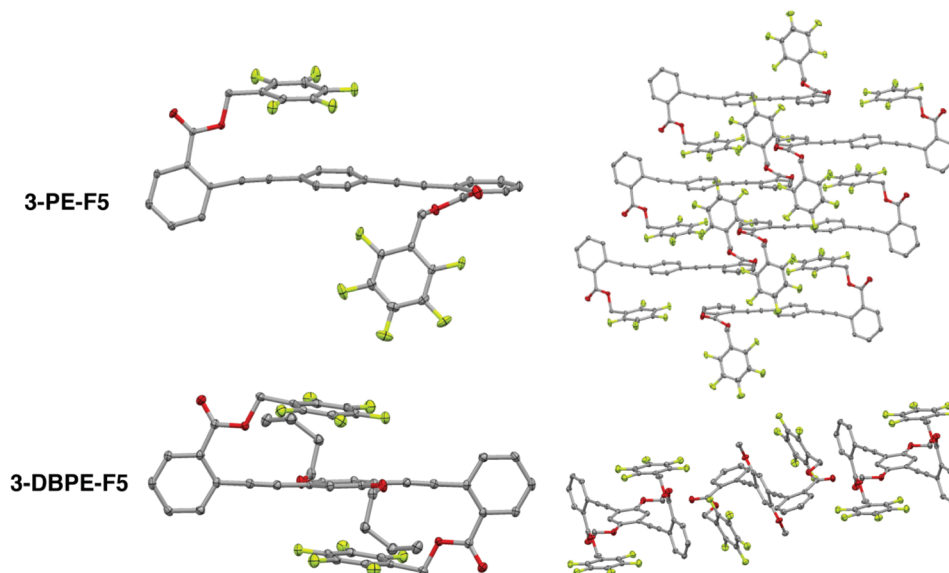


Fig. 3 X-ray crystal structures of **3-PE-F5** (top) and **3-DiOR-PE-F5** (bottom). Hydrogen atoms and outer three carbon atoms of the butoxy chains of **3-DiOR-PE-F5** are omitted for clarity. Thermal ellipsoids are shown at 50% probability.

face of each of the ArF rings stacks with a benzoate ring of another PE. This overall pattern is distinct from the unsubstituted central ring in **3-PE-F5**, which only shows stacking on one face of the central ring. We attribute this difference to the electron-donating capability of the alkoxy substituents on the central ring making the ArF–ArH interactions more favorable. As in other examples, this stacking through the benzylic ester linkers twists the PE linkages, in this case along both alkynes, with torsional angles between 85 and 90°.

Having established the viability of the pentafluorobenzyl *o*-ethynylbenzoate unit as capable of introducing twisting in two different three-ring PEs, we integrated it into the termini of a four-ring PE—**4-PE-F5**—to test the hypothesis that this moiety can twist PE linkages in longer molecules. The crystal structure reveals that each of the two ArF rings stack intramolecularly with ArH rings in the middle of the main chain, with the closest C···C distance of 3.59 Å. The second of the three PE linkages is coplanar, with inter-ring torsional angles of <3°, and these two coplanar arenes stack intramolecularly with neighboring ArF rings on opposite faces of the PE. As in the three-ring PEs, these intramolecular ArF–ArH interactions yield large torsions (78–82°) between the central and terminal PE rings.

A characteristic that four-ring molecules share with our previously reported, terephthalate-based three-ring PEs is an equal number of fluorinated rings and potential stacking partners separated from the benzoate ring by alkynes. Such balancing of the “stoichiometry” of electron-rich and electron-poor arenes introduces the potential for stacks of alternating ArF and ArH rings, similar to that in the cocrystalline solid of hexafluorobenzene and benzene.<sup>39</sup> Among the five different four-ring chromophores we studied, only **4-PE-F5** displayed this feature, with infinite ArF–ArH stacks that propagate along the crystallographic *b* axis. The intermolecular ArF–ArH interactions hold the rings with closest C···C distances <3.5 Å and

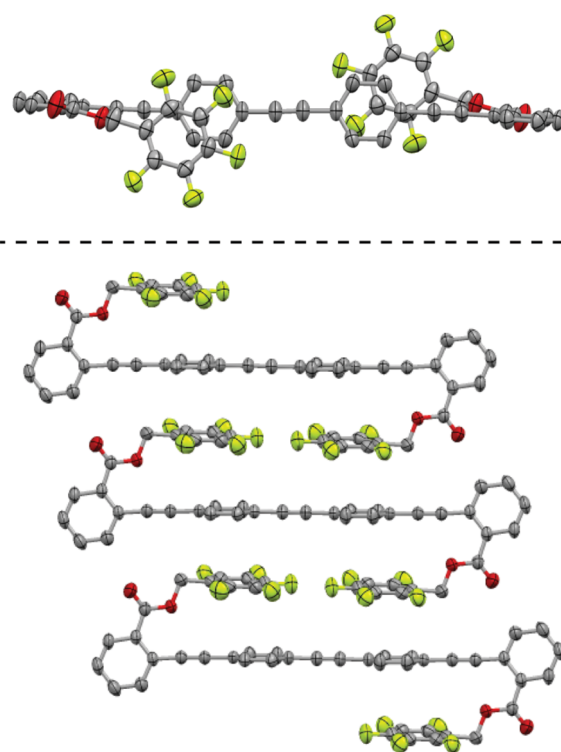


Fig. 4 X-ray crystal structure of an individual molecule (top) and three molecules connected through intramolecular ArF–ArH stacking interactions of **4-PE-F5**. Thermal ellipsoids are shown at 50% probability. Hydrogen atoms are omitted for clarity.

a centroid-to-centroid distance of 3.72 Å, as opposed to 4.18 Å for the intramolecular pairs (Fig. 4).

We also crystallized two analogous compounds that have non-fluorinated benzyl pendants instead of the pentafluorinated rings (Fig. 5). The three-ring PE analog **3-PE-H5** has a crystal

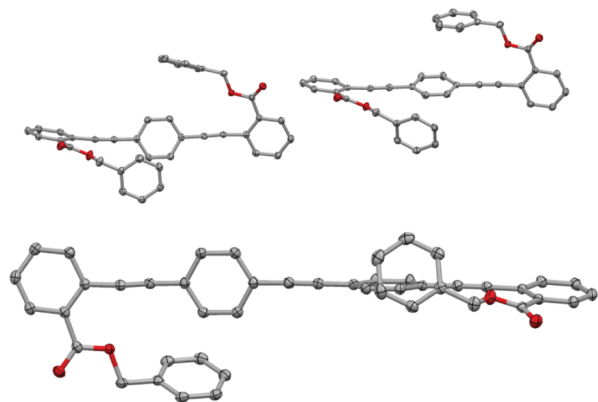


Fig. 5 X-ray crystal structures of **3-PE-H5** (top) and **4-PE-H5** (bottom), each featuring prominent edge–face interactions. Thermal ellipsoids are shown at 50% probability. A disordered  $\text{CHCl}_3$  molecule from the structure of **4-PE-H5** is omitted for clarity, as are hydrogen atoms from both structures.

structure similar to that of **3-PE-F5**, in that one pendant ring interacts cofacially with the central ring, while one does not. Key differences, however, are that the cofacial rings are further apart in this structure (3.7 Å) than in **3-PE-F5**, and that one of the pendant benzyl groups participates in edge–face interactions with the central ring. More strikingly different is the comparison of **4-PE-F5** with its non-fluorinated analog, **4-PE-H5**. Instead of cofacial stacking of pendant and main-chain rings, the pendant rings of **4-PE-H5** undergo edge–face interactions with the central PE rings, allowing PE backbones to interact with each other intermolecularly through edge–face interactions.

**Molecules with central biaryl linkages.** To probe the applicability of this approach to molecules with a greater diversity of linkages, we crystallized four molecules that each have single bonds between two central arenes. As expected based on inter-ring steric interactions, a biphenyl linkage yields a non-planar torsional angle of  $18^\circ$  in **4-BP-F5**, with disorder about the inversion center. Although disordered  $\text{CHCl}_3$  molecules in this particular structure appear to preclude intermolecular stacking of the ArF rings, intramolecular ArF–ArH stacking between the terminal and central rings of the conjugated main chain twists the PE linkages out of planarity by  $77\text{--}85^\circ$ . The ArF ring bends closer to the main chain than in other examples, with  $\text{C}\cdots\text{C}$  distances as close as 3.17 Å.

With the hypothesis that it would result in twisting between each ring along the conjugated backbone, we prepared and crystallized **4-TMBP-F5**. Steric interactions between *ortho*-methyl groups force the central two rings of the biphenyl moiety to be nearly orthogonal, which therefore presents ArH faces that point along different directions for intramolecular interactions with ArF pendants. Although these types of interactions do occur in the crystal structure, the interacting ArF and ArH rings are not fully coplanar and are further separated from each other than in the unmethylated biphenyl derivative, which we attribute to steric repulsion between the ArF rings and methyl groups. Nevertheless, the PE linkages of **4-TMBP-F5** are twisted, with torsional angles of  $62\text{--}66^\circ$  on one side and  $32\text{--}34^\circ$  on the other (Fig. 6).

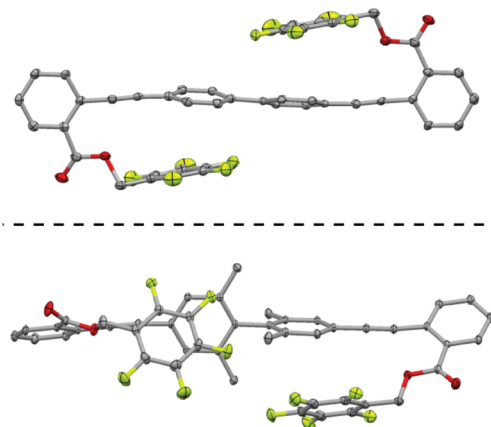


Fig. 6 X-ray crystal structure of biphenyl-based four-ring PEs that show two intramolecular ArF–ArH stacking interactions: **4-BP-F5** (top) and **4-TMBP-F5** (bottom). Thermal ellipsoids are shown at 50% probability. Hydrogen atoms are omitted for clarity.

Two related molecules had highly coplanar biaryl central linkages in the crystal structures. In one example, a 9,9-dimethylfluorene unit enforced coplanar central rings. Intramolecular ArF–ArH interactions occur on only one of the two termini—as seen in **3-PE-F5**, the PE linkage across which the stacking interaction occurs is twisted, with a torsional angle of  $89^\circ$ , while the other side of the 4-ring main chain, which lacks the ArF–ArH stacking, has a torsional angle  $<20^\circ$  (Fig. 7). The ArF rings of this molecule also participate in other, intermolecular cofacial stacking interactions with benzoate rings. Potential explanations for only one intramolecular ArF–ArH interaction occurring

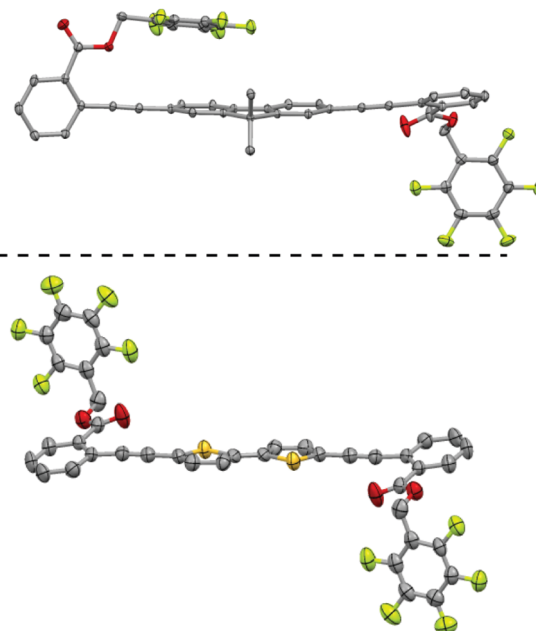


Fig. 7 X-ray crystal structure of four-ring PEs that show one or zero intramolecular ArF–ArH interactions: **4-DMF-F5** (top) and **4-BT-F5** (bottom). Thermal ellipsoids are shown at 50% probability. Hydrogen atoms are omitted for clarity.

Table 1 UV/Vis and fluorescence parameters of all molecules investigated in both dilute CH<sub>2</sub>Cl<sub>2</sub> solution and as solution-cast thin films

Compound	Solution			Thin film		
	$\lambda_{\max}(\text{abs})$ , nm	$\lambda_{\max}(\text{emis})$ , nm	$\Phi_{\text{F}}$	$\lambda_{\max}(\text{abs})$ , nm	$\lambda_{\max}(\text{emis})$ , nm	Emission shift (nm)
3-PE-F5	339	379	0.64	339	406	27
3-PE-H5	338	377	0.76	343	415	38
3-DBPE-F5	378	441	0.71	381	439	-2
4-PE-F5	346	392	0.75	353	403	11
4-PE-H5	348	390	0.94	355	425	35
4-BP-F5	339	391	0.69	335	422	31
4-TMBP-F5	323	377	0.08	324	386	9
4-DMF-F5	361	402	0.77	356	433	31
4-BT-F5	398	461	0.24	396	517	56

include increased steric interactions between the ArF ring and the methyl groups of the fluorene unit, or as we surmised based on the substituent effects in the 3-ring PEs, a decrease in the electrostatic driving force for a second co-facial interaction of the highly coupled arene rings within the fluorene, relative to the observed intramolecular cofacial interactions. Finally, the bithiophene-core derivative **4-BT-F5** lacks any ArF–ArH interactions, which we found somewhat surprising, as ArF–thiophene cofacial stacking interactions have precedent in small conjugated molecules.<sup>40–42</sup> Inter-ring torsions both across each of the alkynes and across the 2,2'-bithiophene unit are less than 20°. Apparently, the energy of interaction between the thiophene and perfluorinated rings is not competitive in this arrangement, an observation that we are currently investigating. Potential explanations are reduced London dispersion forces between the ArF ring and the smaller thiophene rings as compared to ArF–phenyl interactions, or the larger  $\pi$ -orbitals on the sulfur atoms of thiophene rings.

### Optical spectroscopy

UV/Vis absorbance and fluorescence emission spectra of all compounds were obtained both as dilute solutions in CH<sub>2</sub>Cl<sub>2</sub> and as solution-cast thin films (Table 1). In solution, structure–property relationships were consistent with well-established trends in conjugated materials. For example, the spectra of **3-PE-F5** were hypsochromically shifted from the longer yet similarly substituted phenylene–ethynylene **4-PE-F5**. Whether the benzyl pendants were substituted with five fluorine atoms or five hydrogen atoms had virtually no impact on the shape or position of the spectra ( $\Delta\lambda_{\max} \leq 2$  nm) for either **3-PE-F5/H5** or **4-PE-F5/H5**. For the three compounds that have biphenyl linkages between the central rings, the trend of the spectral position correlates with the expected (and crystallographically observed) dihedral angles of the biphenyl units, with the most twisted linkage of **4-TMBP-F5** yielding the most hypsochromically shifted spectra, while the coplanar fluorene linkage is 30–40 nm red-shifted from the tetramethylbiphenyl derivative. The bithiophene derivative has the lowest energy optical spectra of the compounds investigated here—the more electron rich nature of thiophene rings typically yields bathochromically shifted spectra when compared to those of phenyl analogs.<sup>43</sup>

In all compounds, there exist only small differences between the spectra of solids and solutions of these compounds. However, the differences in solid-state packing observed in the

crystal structures lead to important distinctions in the emission spectroscopy of the solution-cast thin films of these compounds. Similarly, there is correlation between the crystal structures and optical properties of the three-ring PEs. The solid-state emission spectrum of **3-DBPE-F5**, the crystal structure of which shows a fully twisted PE backbone, shows almost no shift relative to solution; in contrast, **3-PE-F5** and **3-PE-H5**, the crystal structures of which each show one coplanar linkage along the PE backbones and extensive interactions between the PE chromophore moieties, show 27–38 nm bathochromic shifting when comparing solid to solution emission spectra (Fig. 8).

In examining the four-ring compounds, the most obvious impact of packing comes from simple visual inspection of the luminescence (see the TOC image), which indicates that **4-PE-F5** is obviously more fluorescent than **4-PE-H5**. We estimated the relative quantum yields of fluorescence of the thin films of these two compounds by comparing their fluorescence intensities at indistinguishable absorbance values under otherwise identical experimental conditions (see the ESI†). This experiment indicated that **4-PE-F5** is 5–7× more fluorescent than the hydrogenated analog (Fig. 9). In addition, the weak emission of **4-PE-H5** is bathochromically shifted over 20 nm relative to the spectrum of **4-PE-F5**,

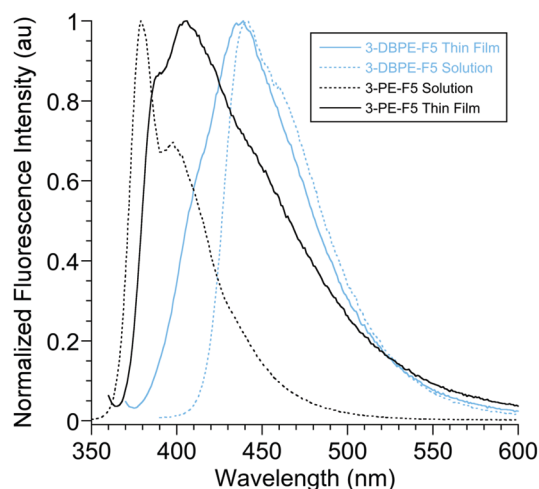


Fig. 8 Height-normalized emission spectra of **3-DBPE-F5** (blue curves) and **3-PE-F5** (black curves) either dissolved in CH<sub>2</sub>Cl<sub>2</sub> (dotted lines) or as drop-cast thin films (solid lines), highlighting the bathochromic shift of **3-PE-F5** that is absent in **3-DBPE-F5**.



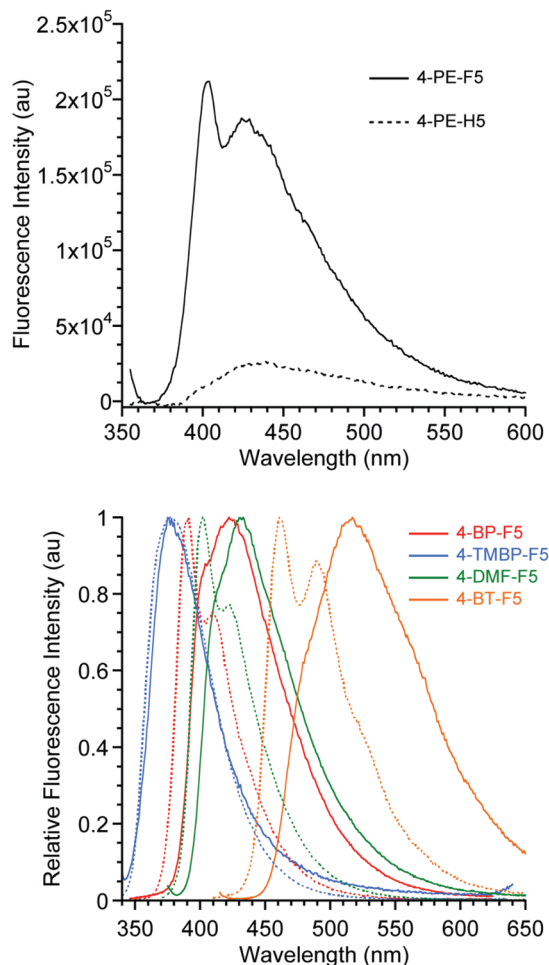


Fig. 9 Fluorescence emission spectra demonstrating select comparisons. Top: Fluorescence emission spectra of thin films of fluorinated and non-fluorinated 4-ring phenylene-ethynylenes, highlighting protection from quenching of **4-PE-F5** by ArF–ArH interactions. The two films show indistinguishable absorbance peaks (0.025) at  $\lambda_{\text{ex}}$  (345 nm). Bottom: Comparison of the solution state (dotted lines) and thin films (solid lines) of the four biaryl-linked four-ring conjugated molecules.

which has a sharp band with the maximum at 403 nm. We attribute these observations to the ArF–ArH cofacial interactions of **4-PE-F5** preventing aggregation and coupling between chromophores that could otherwise yield aggregation-caused quenching. Finally, in comparing the solution-state and solid-state spectra of the four biaryl-linked compounds, the least bathochromically shifted solid-state emission spectrum is assigned to a highly twisted conformation in the solid state (**4-TMBP-F5**). On the other hand, the most bathochromically shifted of the solid-state emission spectra relative to solution is **4-BT-F5**, which we attribute to a combination of interchromophore interactions and coplanarity of the backbone observed in the crystal structure.

## Conclusion

In six of the seven fluorinated compounds described here, intramolecular ArF–ArH stacking interactions between pendant pentafluorobenzyl rings and arenes in the conjugated backbone occur.

Moreover, each example of intramolecular ArF–ArH stacking yields twisting about the ethynyl linkages across which the stacking occurs, including in molecules with four conjugated rings. In the absence of such interactions, however, the conformations of the arylethynyl linkages are unpredictable. ArF–ArH-induced twisting impacts the optoelectronic properties of some of these solids, such as enhanced fluorescence quantum yields or reduced bathochromic shifts when compared to solution.

This work has several important implications for the rational design of conjugated materials. First, it demonstrates the general utility of installing pentafluorobenzyl esters into conjugated materials to twist arylethynyl linkages in the solid state reliably. This work broadens ArF–ArH interactions as a supramolecular synthon to twist PEs both in terms of the length of the conjugated chromophore and the integration of non-alkynyl linkages. Second, it reinforces the potential for electronic substituent effects to increase the likelihood of observing these interactions and programmed twisting, as demonstrated here with the contrast of **3-PE-F5** and **3-DBPE-F5**. Third, conjugated materials that are twisted out of coplanarity exhibit potential inhibition of self-quenching of luminescence, as demonstrated here with **4-PE-H5** and **4-PE-F5**. Therefore, although challenges such as the successful integration of heteroaromatic thiophene-based rings arise, this work demonstrates how discrete, directional aromatic interactions, particularly those involving non-conjugated pendants, can play critical roles in the rational design of the solid-state packing and properties of conjugated materials.

## Conflicts of interest

There are no conflicts to declare.

## Acknowledgements

This work was supported by the Department of Energy, Basic Energy Sciences, through award DE-SC0016423.

## Notes and references

- O. Ostroverkhova, *Chem. Rev.*, 2016, **116**, 13279–13412.
- E. Thanayupong, K. Suttisintong, M. Sukwattanasinitt and N. Niamnont, *New J. Chem.*, 2017, **41**, 4058–4064.
- I. B. Kim, B. Erdogan, J. N. Wilson and U. H. F. Bunz, *Chem. – Eur. J.*, 2004, **10**, 6247–6254.
- H. Jiang, P. Taranekar, J. R. Reynolds and K. S. Schanze, *Angew. Chem., Int. Ed.*, 2009, **48**, 4300–4316.
- Y. Tang, T. S. Corbitt, A. Parthasarathy, Z. Zhou, K. S. Schanze and D. G. Whitten, *Langmuir*, 2011, **27**, 4956–4962.
- H. C. Pappas, S. Phan, S. Yoon, L. E. Edens, X. Meng, K. S. Schanze, D. G. Whitten and D. J. Keller, *ACS Appl. Mater. Interfaces*, 2015, **7**, 27632–27638.
- Y. Wang, K. S. Schanze, E. Y. Chi and D. G. Whitten, *Langmuir*, 2013, **29**, 10635–10647.
- H. Masai, T. Fujihara, Y. Tsuji and J. Terao, *Chem. – Eur. J.*, 2017, **23**, 15073–15079.

- 9 J.-T. Zheng, R.-W. Yan, J.-H. Tian, J.-Y. Liu, L.-Q. Pei, D.-Y. Wu, K. Dai, Y. Yang, S. Jin, W. Hong and Z.-Q. Tian, *Electrochim. Acta*, 2016, **200**, 268–275.
- 10 Q. Lu, K. Liu, H. Zhang, Z. Du, X. Wang and F. Wang, *ACS Nano*, 2009, **3**, 3861–3868.
- 11 J. K. Mwaura, M. R. Pinto, D. Witker, N. Ananthakrishnan, K. S. Schanze and J. R. Reynolds, *Langmuir*, 2005, **21**, 10119–10126.
- 12 G. Adam, T. Yohannes, M. White, A. Montaigne, C. Ulbricht, E. Bircckner, S. Rathgeber, C. Kästner, H. Hoppe, N. S. Sariciftci and D. A. M. Egbe, *Macromol. Chem. Phys.*, 2014, **215**, 1473–1484.
- 13 D. A. M. Egbe, S. Türk, S. Rathgeber, F. Kühnlenz, R. Jadhav, A. Wild, E. Bircckner, G. Adam, A. Pivrikas, V. Cimrova, G. Knör, N. S. Sariciftci and H. Hoppe, *Macromolecules*, 2010, **43**, 1261–1269.
- 14 K. Okuyama, T. Hasegawa, M. Ito and N. Mikami, *J. Phys. Chem.*, 1984, **88**, 1711–1716.
- 15 J. M. Seminario, A. G. Zacarias and J. M. Tour, *J. Am. Chem. Soc.*, 1998, **120**, 3970–3974.
- 16 D. Yan and D. G. Evans, *Mater. Horiz.*, 2014, **1**, 46–57.
- 17 S. Varghese and S. Das, *J. Phys. Chem. Lett.*, 2011, **2**, 863–873.
- 18 M. D. Curtis, J. Cao and J. W. Kampf, *J. Am. Chem. Soc.*, 2004, **126**, 4318–4328.
- 19 S. Menning, M. Krämer, B. A. Coombs, F. Rominger, A. Beeby, A. Dreuw and U. H. F. Bunz, *J. Am. Chem. Soc.*, 2013, **135**, 2160–2163.
- 20 G. Brizius, K. Billingsley, M. D. Smith and U. H. F. Bunz, *Org. Lett.*, 2003, **5**, 3951–3954.
- 21 A. Beeby, K. S. Findlay, A. E. Goeta, L. Porrès, S. R. Rutter and A. L. Thompson, *Photochem. Photobiol. Sci.*, 2007, **6**, 982–986.
- 22 J.-S. Yang, J.-L. Yan, C.-Y. Hwang, S.-Y. Chiou, K.-L. Liao, H.-H. Gavin Tsai, G.-H. Lee and S.-M. Peng, *J. Am. Chem. Soc.*, 2006, **128**, 14109–14119.
- 23 C. Rest, R. Kandaneli and G. Fernández, *Chem. Soc. Rev.*, 2015, **44**, 2543–2572.
- 24 A. Mukherjee, *Cryst. Growth Des.*, 2015, **15**, 3076–3085.
- 25 W. Hu, N. Zhu, W. Tang and D. Zhao, *Org. Lett.*, 2008, **10**, 2669–2672.
- 26 E. A. Meyer, R. K. Castellano and F. Diederich, *Angew. Chem., Int. Ed.*, 2003, **42**, 1210–1250.
- 27 J. W. Hwang, P. Li and K. D. Shimizu, *Org. Biomol. Chem.*, 2017, **15**, 1554–1564.
- 28 F. Ponzini, R. Zagha, K. Hardcastle and J. S. Siegel, *Angew. Chem., Int. Ed.*, 2000, **39**, 2323–2325.
- 29 R. Xu, W. B. Schweizer and H. Frauenrath, *Chem. – Eur. J.*, 2009, **15**, 9105–9116.
- 30 Y. Sakamoto, T. Suzuki, M. Kobayashi, Y. Gao, Y. Fukai, Y. Inoue, F. Sato and S. Tokito, *J. Am. Chem. Soc.*, 2004, **126**, 8138–8140.
- 31 Y. Sakamoto and T. Suzuki, *J. Org. Chem.*, 2017, **82**, 8111–8116.
- 32 R. H. Pawle, T. E. Haas, P. Müller and S. W. Thomas, III, *Chem. Sci.*, 2014, **5**, 4184–4188.
- 33 S. A. Sharber, R. N. Baral, F. Frausto, T. E. Haas, P. Müller and S. W. Thomas, III, *J. Am. Chem. Soc.*, 2017, **139**, 5164–5174.
- 34 S. A. Sharber, K.-C. Shih, A. Mann, F. Frausto, T. E. Haas, M.-P. Nieh and S. W. Thomas, *Chem. Sci.*, 2018, **9**, 5415–5426.
- 35 W. H. Melhuish, *J. Phys. Chem.*, 1961, **65**, 229–235.
- 36 M. Jean, J. Renault, P. van de Weghe and N. Asao, *Tetrahedron Lett.*, 2010, **51**, 378–381.
- 37 M. A. Fox, J. A. K. Howard, J. A. H. MacBride, A. Mackinnon and K. Wade, *J. Organomet. Chem.*, 2003, **680**, 155–164.
- 38 D. Vonlanthen, J. Rotzler, M. Neuburger and M. Mayor, *Eur. J. Org. Chem.*, 2010, 120–133.
- 39 J. H. Williams, J. K. Cockcroft and A. N. Fitch, *Angew. Chem., Int. Ed. Engl.*, 1992, **31**, 1655–1657.
- 40 D. M. Cho, S. R. Parkin and M. D. Watson, *Org. Lett.*, 2005, **7**, 1067–1068.
- 41 A. Facchetti, M. H. Yoon, C. L. Stern, H. E. Katz and T. J. Marks, *Angew. Chem., Int. Ed.*, 2003, **42**, 3900–3903.
- 42 M. H. Yoon, A. Facchetti, C. E. Stern and T. J. Marks, *J. Am. Chem. Soc.*, 2006, **128**, 5792–5801.
- 43 X. Zhang, H. Yu and Y. Xiao, *J. Org. Chem.*, 2012, **77**, 669–673.